

THE PENNSYLVANIA STATE UNIVERSITY
SCHREYER HONORS COLLEGE

DEPARTMENT OF BIOLOGY

ANALYZING THE EFFECTS OF DISRUPTING XYLAN ACETYLATION IN
BRACHYPODIUM DISTACHYON

JUSTIN SLOVIN
SPRING 2018

A thesis
submitted in partial fulfillment
of the requirements
for a baccalaureate degree
in Biology
with honors in Biology

Reviewed and approved* by the following:

Charles T. Anderson
Assistant Professor of Biology
Thesis Supervisor

Daniel Cosgrove
Professor and Holder of the Eberly Chair in Biology
Honors Adviser

* Signatures are on file in the Schreyer Honors College.

ABSTRACT

Plant cell walls are critical for growth and development, and also store carbon as energy rich, renewable biomaterial. Xylan is one of the principle structural hemicelluloses in the cell walls of most species of plants, including the model eudicot *Arabidopsis thaliana* and the model grass *Brachypodium distachyon*. Xylan acetylation, which is thought to be important for the interactions between xylan and other cell wall polysaccharides and can inhibit processing of cell walls for bioenergy production, is mediated by the acetyltransferase TRICHOME BIREFRINGENCE-LIKE 29 (TBL29), as well as TBL34 and TBL35. Affecting the expression of these genes decreases the overall amount of xylan acetylation in *Arabidopsis thaliana*, but homologs of these genes have not yet been functionally characterized in *Brachypodium*. Using both microRNA knockdown and CRISPR/Cas9 gene knockout methods, the expression of *TBL29*, *TBL34*, and *TBL35* was interrupted. The results of growth experiments indicate that knocking out these genes results in stunted plants and drought stress symptoms in certain transformant lines, whereas knocking down the *TBL29* gene does not result in stunting or drought stress symptoms through the T1 generation. The findings from this study lead to hope of being able to discover how the *Brachypodium distachyon* cell wall differs from the *Arabidopsis thaliana* cell wall, and how impeding xylan acetylation affects both organisms.

TABLE OF CONTENTS

LIST OF FIGURES	iii
LIST OF TABLES	iv
ACKNOWLEDGEMENTS	v
Chapter 1 Introduction	1
Chapter 2 Materials and Methods	11
Chapter 3 <i>TBL29</i> microRNA Plants Do Not Show Significant Stunting Compared To Control Plants	17
<i>TBL29</i> microRNA T1 Height Measurements Show No Significant Stunting Compared To <i>GFP</i> microRNA T1 Height Measurements.....	18
Chapter 4 <i>TBL29</i> CRISPR Plants Show Some Significant Stunting Compared To <i>GFP</i> CRISPR Plants.....	20
<i>TBL29</i> CRISPR T1 Height Data Shows Some Significant Stunting Compared To <i>GFP</i> CRISPR T1 Height Data	20
Chapter 5 <i>TBL29/34/35</i> CRISPR Plants Show Some Stunting, As Well As Increased Lethality And Drought Stress Symptoms, Compared To <i>GFP</i> CRISPR Plants...	22
T0 Generation Survivability Results Show Increased Lethality In <i>TBL29/34/35</i> CRISPR Plants, When Compared To <i>GFP</i> CRISPR Plants	23
T1 Height Data Shows Some Stunting In <i>TBL29/34/35</i> CRISPR Lines Compared To <i>GFP</i> CRISPR Lines	25
Sequencing Data Shows The Correlation Between Mutations In <i>TBL29</i> , <i>34</i> , and <i>35</i> And Stunted Growth	26
Structural Comparison Shows Drought Stress Symptoms In <i>TBL29/34/35</i> CRISPR Plants But Not <i>GFP</i> CRISPR Plants.....	27
Chapter 6 Discussion	30
Chapter 7 Conclusion.....	36
BIBLIOGRAPHY	37

LIST OF FIGURES

- Figure 1: Representation of xylan. Black hexagons represent the xylose residues, while the red triangles, orange quadrilaterals, and blue circles represent glucuronic acid, acetyl, and arabinose side chains respectively. The green pentagons represent methylglucuronic acid side chains. Figure adapted from (Rennie and Scheller, 2014).....3
- Figure 2: Phylogenic tree showing the inferred evolutionary relationships of *TBL29* across different plant species. The orthologs for the three organisms mentioned in this paper (*Brachypodium distachyon*, *Arabidopsis thaliana*, and *Oryza sativa*) are labeled with blue text. Image collected from PlantTribes database (Wall et al., 2007) and (Petrik, personal communication). Species Abbreviations: Aquco – *Aquilegia coerulea*, Nelnu – *Nelumbo nucifera*, Frave – *Fragaria vesca*, Poptr – *Populus trichocarpa*, Theca – *Theobroma cacao*, Carpa – *Carica papaya*, Thepa – *Thellungiella parvula*, Arath – *Arabidopsis thaliana*, Mingu – *Mimulus guttatus*, Soltu – *Solanum tuberosum*, Solly – *Solanum lycopersicum*, Glyma – *Glycine max*, Medtr – *Medicago truncatula*, Vitvi – *Vitis vinifera*, Phoda – *Phoenix dactylifera*, Musac – *Musa acuminata*, Orysa – *Oryza sativa*, Bradi – *Brachypodium distachyon*, Sorbi – *Sorghum bicolor*, Ambtr – *Amborella trichopoda*5
- Figure 3: Phylogenic tree showing the inferred evolutionary relationships of *TBL34* across different plant species. The orthologs for the three organisms mentioned in this paper (*Brachypodium distachyon*, *Arabidopsis thaliana*, and *Oryza sativa*) are labeled with blue text. Image collected from PlantTribes database (Wall et al., 2007) and (Petrik, personal communication). Same species abbreviations apply as for Figure 2.6
- Figure 4: Phylogenic tree showing the inferred evolutionary relationships of *TBL35* across different plant species. The orthologs for the three organisms mentioned in this paper (*Brachypodium distachyon*, *Arabidopsis thaliana*, and *Oryza sativa*) are labeled with blue text. Image collected from PlantTribes database (Wall et al., 2007) and (Petrik, personal communication). Same species abbreviations apply as for Figure 2.7
- Figure 5: Schematic of *BdTBL29* gene showing the positions of both guideRNAs (gRNA 1 and Possible gRNA2) used for CRISPR construct design, as well as positions of primers (1-4) used for genotyping and sequencing.13
- Figure 6: Schematic of *BdTBL34* gene showing the positions of the guideRNA (gRNA1) used for CRISPR construct design, as well as positions of primers (Primer Forward and New R Primer) used for genotyping and sequencing. Primer R was initially designed for genotyping, but did not work well.13
- Figure 7: Schematic of *BdTBL35* gene showing the positions of the guideRNA (GRNASEquenceTBL35) used for CRISPR construct design, as well as positions of primers (Primer F and Primer R) used for genotyping and sequencing.13
- Figure 8: *TBL29* amiRNA Height Data. Most of the TBL lines contained between 8 and 10 plants (lines 64B and 64C only had four surviving seed from the T0 generation). These plants were compared to *GFP* amiRNA lines containing between 8 and 12 plants per sample. No significant differences between plant heights were detected ($p > 0.05$, T-test).18

- Figure 9: TBL29 CRISPR Height Data. The four surviving CRISPR lines (ten plants each) were compared to two *GFP* CRISPR lines (total of 11 plants). Error bars represent standard deviation. Asterisks (*) indicate significant difference from the GFP control ($p < 0.05$, T-test).....21
- Figure 10 *TBL29/34/35* Triple CRISPR Height Data. The three surviving triple CRISPR lines (ten plants each) were compared to two *GFP* CRISPR lines (total of 11 plants). Error bars represent standard deviation. Asterisks (*) indicate significant difference from the GFP control ($p < 0.05$, T-test).25
- Figure 11: Two pots of *TBL29/34/35* CRISPR T1 line 161A plants compared to plants from the *GFP* control.....27
- Figure 12: Photograph of stem of plant number 2 from *TBL29/34/35* CRISPR line 161A showing stunting and drought-like phenotypes. A large number of leaves and stems from this line were thinner and showed different coloration than both *GFP* CRISPR controls and other *TBL29/34/35* CRISPR lines.28
- Figure 13: Photograph of stem from plant number 6 of *GFP* CRISPR Control. This stem represents the non-stunted, non-drought phenotype.28
- Figure 14: Expression profile of TBL29, showing which parts of the plant anatomy express TBL29 at the highest levels. (Petrik, 2018)31

LIST OF TABLES

Table 1: microRNA sequences used to knock down <i>TBL29</i> expression in <i>Brachypodium distachyon</i>	11
Table 2: CRISPR sequences used to knock out <i>TBL29</i> , <i>TBL34</i> , and <i>TBL35</i> expression in <i>Brachypodium distachyon</i>	12
Table 3: <i>TBL29/34/35</i> CRISPR T0 Generation Results. This table shows the fate of each of the <i>TBL29/34/35</i> CRISPR lines that survived through tissue culture and were planted. Each transformant was assigned a number for survivability, with 0 meaning that the transformant died, 0.5 meaning that the transformant lived, but produced no usable seed, and 1 meaning that the transformant lived and produced seed.	23
Table 4: <i>GFP</i> CRISPR T0 Generation Results. This table shows the fate of each of the <i>GFP</i> CRISPR control lines that survived through tissue culture and were planted. Survivability scale is the same as the scale used in Table 3.	23
Table 5: Sequencing data for stunted <i>TBL29/34/35</i> Triple CRISPR plants and <i>GFP</i> control. The plants were each identified by their line and plant number, as well as what the sequencing data showed at each locus of interest.	26

ACKNOWLEDGEMENTS

I would like to thank my research mentors, Dr. Charles T. Anderson and Dr. Deborah Petrik, for training me in experimental technique and guiding me throughout this entire process, as well as Dr. Daniel Cosgrove for his helpful comments on my thesis drafts. I would also like to thank the other members of the Anderson Lab who helped me with my research: Will Barnes, Yue Rui, Yintong Chen, and Benjamin Ratchford. Additionally, I would like to thank the Center for Lignocellulose Structure and Formation (CLSF) and the Pennsylvania State Department of Biology for assisting with funding for this project. Finally, I would like to thank my family and friends for supporting me throughout this entire process. This work was supported as part of The Center for Lignocellulose Structure and Formation, an Energy Frontier Research Center funded by the U.S. Department of Energy, Office of Science, Basic Energy Sciences under Award # DE-SC0001090.

Chapter 1

Introduction

The state of the environment is one of the chief concerns when discussing threats to humanity on a global scale. Recent predictions project that nearly ten percent of species will be forced into extinction due to climate change (Javeline et al., 2015). Moreover, estimates show that, among other areas, the American Midwest will likely become too warm to sustain crop production into the twenty-second century (Sommer, 2015). The primary reason for this is greenhouse gas accumulation in the atmosphere, largely due to the burning of fossil fuels (Withagen, 1994). To counteract this, many projects working to discover alternative sources of energy are underway, including those looking into renewable energy in the form of biofuel production from plants (Carroll and Somerville, 2009).

There are many reasons that biofuels are being researched heavily, besides the fact that they are much more beneficial to the environment than fossil fuels. Chief among these is the renewability and efficiency of biofuels. Due to the fact that many biofuels are derived from plant biomass, every new generation of plants can replace the energy provided by the previous generation, and certain bioenergy feedstocks can even be grown on land thought to be unsuitable for agriculture (Nigam and Singh, 2011). However, most current biofuels are made from edible plant polysaccharides, such as starch and sucrose. Recent research has discussed how to use other plant polysaccharides, such as cellulose and the various cell wall hemicelluloses for biofuel production. This is because making biofuels out of starches cuts into the amount of food that can be produced by the same crops (Tilman et al, 2009). Starch is present in high amounts in certain

crops, such as corn, peas, potatoes, and rice; but it is also used in many foods as a thickening agent, including pudding and gravy. Additionally, starch can be fermented, and used in alcoholic beverages (Eliasson, 2004). A significant drop in food or beverage production might occur if large amounts of starch are suddenly used for widespread fuel production. Using the inedible parts of plants (such as celluloses and hemicelluloses) for biofuel production would be much more efficient, both for food production and for energy production (Naik et al., 2010), but the relatively high cost of obtaining usable sugars from plant cell walls has hindered the ability for this new “lignocellulosic biofuel” market to gain traction in the global economy.

One major hemicellulose group is the xylans, principle structural hemicelluloses found in all plants. For the purpose of this introduction, plants will be divided into two categories: those with type I cell walls (eudicots and non-grass monocots) and those with type II cell walls (typically grasses). Plants with type I cell walls, such as the eudicot *Arabidopsis thaliana*, have primary walls composed mainly of pectins, xyloglucan, and cellulose, with xylan being present mainly in their secondary cell walls. Secondary cell walls are usually thickened and located between the plasma membrane and the primary cell wall and function primarily in plant tissue rigidity. Plants with type II cell walls, such as *Brachypodium distachyon*, have xylan in both their primary and secondary cell walls. Primary cell walls are the outermost layer of the plant cell and are synthesized by growing cells. Primary cell walls are typically much more flexible than secondary cell walls, as they must be able to expand with the cell, in the presence of water, as it grows (Cosgrove and Jarvis, 2012).

Structurally, xylan is a polymer with a backbone of xylose molecules connected via a beta 1-4 linkage. The backbone is thought to be built by a large group of glycosyltransferase enzymes. Most of these enzymes are named after the phenotype that they cause if they are

knocked out in *Arabidopsis thaliana*: irregular xylem (*irx*). *IRX9*, *IRX10*, and *IRX14*, as well as the irregular xylem-like genes *IRX9-L*, *IRX10-L*, and *IRX14-L*, are involved in the elongation of the xylan chain (Brown et al., 2007 and Rennie and Scheller, 2014). Additionally, xylan can be substituted with a large number of side chains, including acetyl groups, glucuronic acid groups, arabinose groups, and methylglucuronic acid groups (Rennie and Scheller, 2014) (Figure 1).

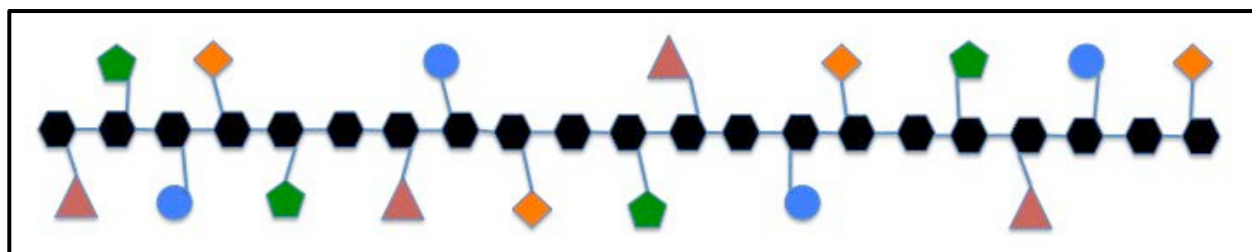


Figure 1: Representation of xylan. Black hexagons represent the xylose residues, while the red triangles, orange quadrilaterals, and blue circles represent glucuronic acid, acetyl, and arabinose side chains respectively. The green pentagons represent methylglucuronic acid side chains. Figure adapted from (Rennie and Scheller, 2014).

Acetyl groups are usually found on the O-2 and O-3 residues in xylose residues, as well as along the backbones and/or side chains of other plant polysaccharides, including the pectins homogalacturonan and rhamnogalacturonan, as well as mannan and xyloglucan (Manabe et al., 2011). Glucuronic acid substitution is thought to be regulated by the GLUCURONIC ACID SUBSTITUTION OF XYLAN (GUX) family of genes, *GUX1* and *GUX2* (Rennie and Scheller, 2014). The two GUX gene products are thought to act independently, with *GUX1* spacing glucuronic acid residues evenly between 6-26 xylose sugars apart, and *GUX2* spacing residues either oddly or evenly (Bromley et al., 2013, Rennie and Scheller, 2014). Arabinose is a diastereomer of xylose, and as a side chain influences interactions between xylan and other cell wall polysaccharides (Caballero et al., 2003). Some glucuronic acids are modified to form O-4 methylated glucuronic acid. In *Arabidopsis thaliana*, it is thought that the

GLUCURONOXYLAN METHYLTRANSFERASE (GXMT) family of genes is responsible for this methylation (Urbanowicz et al., 2012).

Of those side chains, the acetyl chains present the most research interest for this project. Xylan acetylation is thought to be regulated by TRICHOME BIREFRINGENCE-LIKE 29 (TBL29) (Rennie and Scheller, 2014). TBL29 is thought to code for an acetyltransferase containing a Domain of Unknown Function (DUF): DUF 231. Proteins containing this domain have been linked to acetylation of other cell wall polysaccharides, including xyloglucan (Gille et al., 2011). Previous studies estimate that *Arabidopsis thaliana* plants lacking functional *TBL29* genes have up to a 40% decrease in xylan acetylation (Yuan et al., 2016). Further studies have indicated that inactivation of two other genes, *TBL34* and *TBL35*, in addition to inactivating *TBL29*, causes an even larger decrease in acetylation in *Oryza sativa* (Gao et al., 2017) and in *Arabidopsis thaliana* (Yuan et al., 2016). Figures 2-4 show the putative phylogenetic relationships between TBL29, 34, and 35 in *Arabidopsis thaliana*, *Brachypodium distachyon*, and *Oryza sativa*. The genes have a very recent common ancestor in *Brachypodium distachyon* and *Oryza sativa*, while the common ancestor of the genes in *Arabidopsis thaliana* is much more distant. These trees provide important context for viewing the *Brachypodium distachyon* genes involved in this project and explain why the papers involving genes from *Arabidopsis thaliana* and *Oryza sativa* were considered important resources. The *Arabidopsis thaliana* genome was sequenced in 2000 (The Arabidopsis Genome Initiative, 2000), and the *Oryza sativa* genome was first sequenced in 2005 (International Rice Genome Sequencing Project, 2005). The *Brachypodium distachyon* genome was not fully sequenced until 2010 (The International Brachypodium Initiative, 2010). This indicates that research on other model organisms has been

underway for much longer. Therefore, the best way to find direction for research into

Brachypodium distachyon is to look to what research was performed on related organisms.

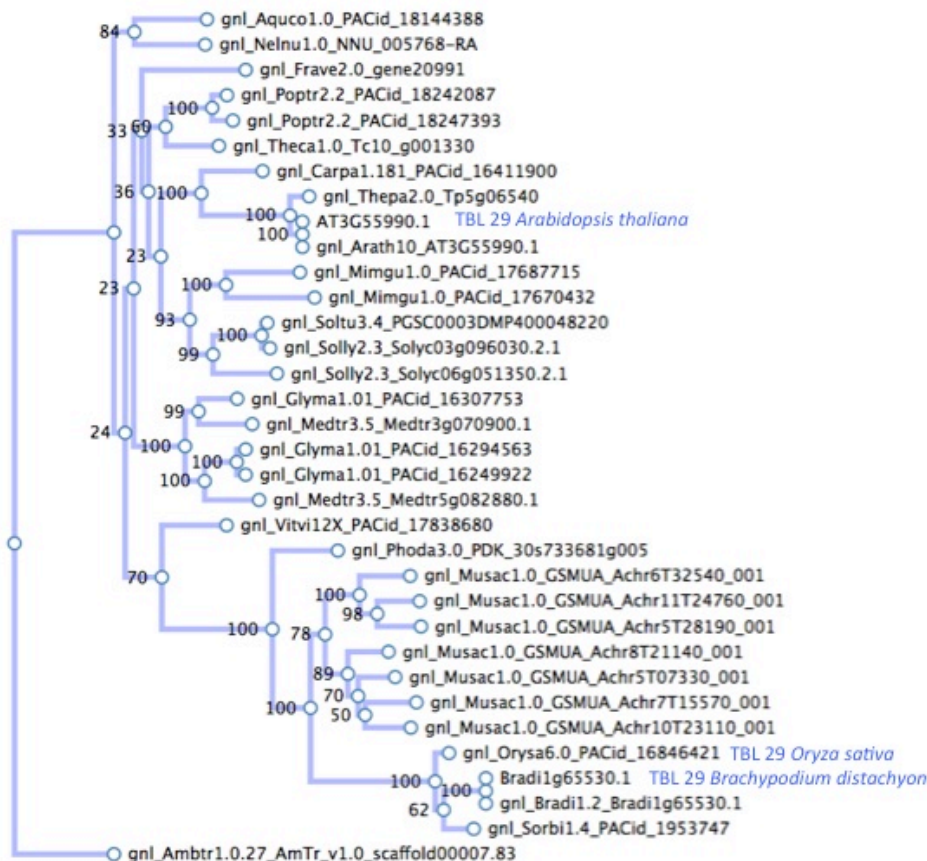


Figure 2: Phylogenetic tree showing the inferred evolutionary relationships of *TBL29* across different plant species. The orthologs for the three organisms mentioned in this paper (*Brachypodium distachyon*, *Arabidopsis thaliana*, and *Oryza sativa*) are labeled with blue text. Image collected from Plant Tribes database (Wall et al., 2007) and (Petrik, personal communication). Species Abbreviations: Aquco – *Aquilegia coerulea*, Nelnu – *Nelumbo nucifera*, Frave – *Fragaria vesca*, Poptr – *Populus trichocarpa*, Theca – *Theobroma cacao*, Carpa – *Carica papaya*, Thepa – *Thellungiella parvula*, Arath – *Arabidopsis thaliana*, Mimgu – *Mimulus guttatus*, Soltu – *Solanum tuberosum*, Solly – *Solanum lycopersicum*, Glyma – *Glycine max*, Medtr – *Medicago truncatula*, Vitvi – *Vitis vinifera*, Phoda – *Phoenix dactylifera*, Musac – *Musa acuminata*, Orysa – *Oryza sativa*, Bradi – *Brachypodium distachyon*, Sorbi – *Sorghum bicolor*, Ambtr – *Amborella trichopoda*

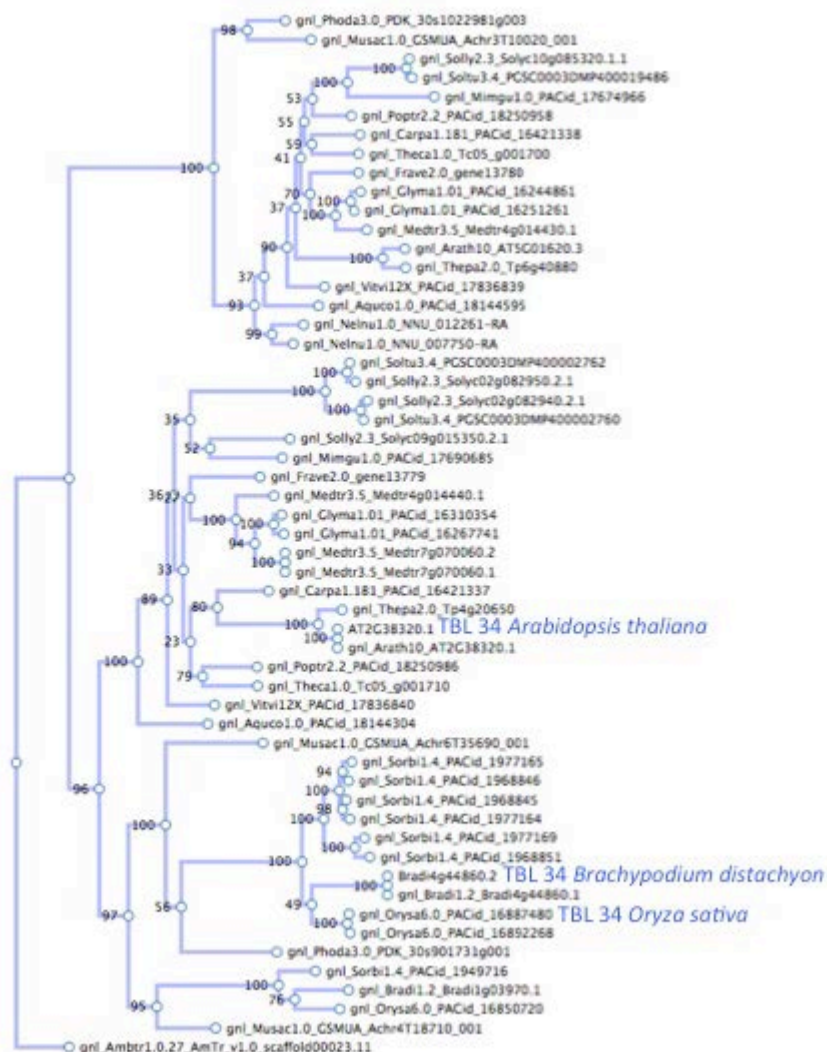


Figure 3: Phylogenetic tree showing the inferred evolutionary relationships of *TBL34* across different plant species. The orthologs for the three organisms mentioned in this paper (*Brachypodium distachyon*, *Arabidopsis thaliana*, and *Oryza sativa*) are labeled with blue text. Image collected from Plant Tribes database (Wall et al., 2007) and (Petrik, personal communication). Same species abbreviations apply as for Figure 2.

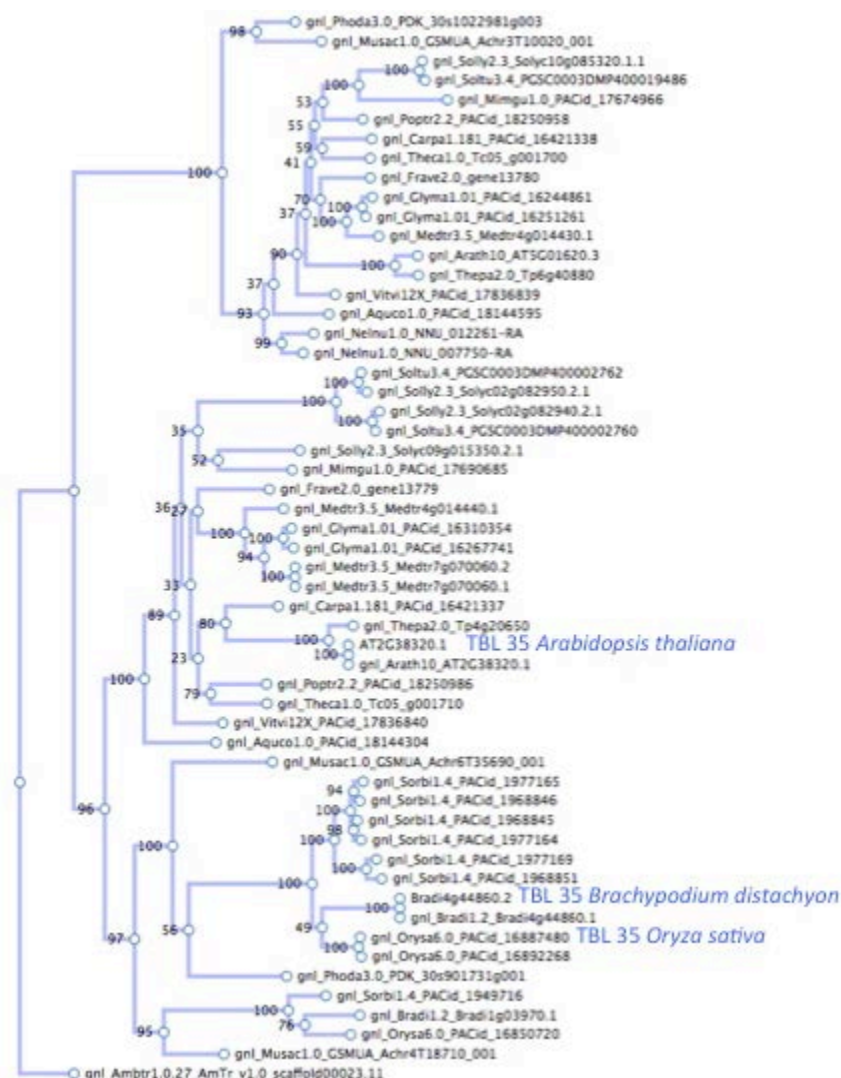


Figure 4: Phylogenetic tree showing the inferred evolutionary relationships of *TBL35* across different plant species. The orthologs for the three organisms mentioned in this paper (*Brachypodium distachyon*, *Arabidopsis thaliana*, and *Oryza sativa*) are labeled with blue text. Image collected from PlantTribes database (Wall et al., 2007) and (Petrik, personal communication). Same species abbreviations apply as for Figure 2.

The ability to manipulate xylan acetylation levels has many potential benefits. For example, acetyl groups often delay biofuel production, because biofuel producing organisms, such as yeast, often have slower fermentation processes when exposed to acetate (Weng et al., 2008). This makes producing plants with less acetylated xylan a coveted prospect, but there are some negatives to this process as well. Despite the benefit of increased biofuel production

efficiency, the change in xylan structure in *tbl29* mutants also causes them to exhibit collapsed xylem vessels, leading to drought stress symptoms, including stunted growth (Bensussan et al., 2015). This has the potential to cause a phenotypic “trade off,” where large amounts of difficult-to-digest biomass are traded for much smaller amounts of easy-to-digest biomass. This makes the idea of producing plants with similar amounts of biomass to the wild type plants, but less acetylated xylan than the wild type plants, a potentially valuable idea. This was attempted in *Arabidopsis thaliana*, but not in *Brachypodium distachyon*. Researchers used ethyl methanesulfonate, a compound that induces DNA mispairing by undergoing SN₁ and SN₂ reactions with guanine bases (Sega, 1984), to induce mutations across *Arabidopsis tbl29* knockout lines (Bensussan et al., 2015). They were able to screen for the lines that showed normal growth and height measurements and discovered that these lines had acquired a second mutation in the *KAKTUS* (KAK) gene that suppressed the stunted growth and collapsed xylem phenotypes (Bensussan et al., 2015). The KAK gene is thought to affect trichome development, regulating endoreduplication (the replication of the nuclear genome without cell division) and ensuring that trichome branching is limited (El Refy et al., 2003). Additionally, it is thought to play a role in vascular development (Bensussan et al., 2015). A project like this is more of a long term goal, than a realistic goal for this particular project, however, as much more is known about the *Arabidopsis thaliana* cell wall than the *Brachypodium distachyon* cell wall, although some studies of cell wall composition in *Brachypodium* have been reported (Rancour and Marita, 2012; Rancour et al., 2015; Cass et al., 2015). Before attempting to create lines with multiple cell wall mutations, a fundamental understanding of the *Brachypodium distachyon* cell wall is critical.

The primary goal of this project is to determine whether *Brachypodium distachyon* responds similarly to *Arabidopsis thaliana* when xylan acetylation is perturbed. Due to the fact that xylan is abundant in both primary and secondary cell walls in *Brachypodium distachyon*, compared to its presence mainly in secondary walls in *Arabidopsis thaliana*, and the two organisms have different cell wall compositions (Vogel, 2008), there is no guarantee that the organisms will share common phenotypes. One piece of information motivating the investigation of xylan acetylation in *Brachypodium* is that stunting and drought stress phenotypes were seen in mutants of another grass species, *Oryza sativa*, lacking xylan acetylation (Gao et al., 2017). A potential application of this project is determining whether it is possible to reduce xylan acetylation, without causing drought stress symptoms. This might allow for more efficient biofuel production and assist in any potential energy crisis, as well as helping to reduce humanity's substantial carbon footprint.

The interruption of xylan acetylation was accomplished in two different ways for this project: genetic editing via CRISPR/Cas9 and microRNA. Both of these tactics were designed to reduce the functionality of *TBL* genes in *Brachypodium distachyon*, but they work in different ways. The CRISPR/cas9 system often completely inactivates target genes. If the desired effect is reduced gene expression without full knockout, microRNA is used. Rather than regulating gene expression prior to transcription, microRNAs limit gene expression prior to translation by targeting mRNA for degradation or by directly inhibiting translation (He and Hannon, 2004). The CRISPR/Cas9 system uses two primary components to target genes: guide RNA (gRNA) corresponding to the desired target sequences in the genome, and a Cas9 nuclease. The Cas9 nuclease can interact with this gRNA and cause a double strand break in the genome, which is often repaired via non-homologous end joining, causing a mutation between the third and fourth

bases in the target sequence. The desired outcome of this mechanism is the insertion or deletion of one or more nucleotides from the genome, leading to a frameshift mutation, the loss or gain of an amount of bases unequal to a multiple of three (removing/adding a number of bases equal to a multiple of three will only remove/add a certain number of intact codons from the amino acid sequence, which could potentially keep the protein relatively intact) (Sandler and Joung, 2014).

Another goal of this project is to determine whether the interactions between the newly modified xylan and cellulose are changed in any way. Xylan and its interactions with cellulose have profound effects on cell wall integrity. In *Arabidopsis thaliana*, decreased xylan levels can lead to weakened cell walls and defects in vascular development (Simmons et al., 2016). This raises the question of whether modified xylan will have similar effects. It is thought that, in solution, xylan forms a threefold helical screw, meaning that it will twist a full 360 degrees every three glycosidic linkages (Grantham et al., 2017). Despite this, in the presence of cellulose, this structure becomes a twofold helical screw, twisting a full 360 degrees after only two glycosidic linkages. It is hypothesized that hydrogen bonding between cellulose and xylan causes this structural change, so the loss of the potential hydrogen bonding methyl and ketone groups from xylan might impact these interactions. However, it is also thought that methylglucuronic acid groups become more plentiful in acetyl group-deficient xylan, which could lead to a restoration of potential xylan-cellulose hydrogen bonding (Grantham et al., 2017).

Chapter 2

Materials and Methods

MicroRNA Construct Design – Artificial micro RNA (amiRNA) constructs were designed using the James Carrington lab’s Plant Small RNA Maker Suite Web App (Fahlgren et al., 2016) and assembled using a published protocol (Carbonell et al., 2014). This protocol was selected for its ability to quickly generate micro RNA constructs in a cost effective manner. The construct was created by annealing two partially complementary small nucleotide sequences, each targeting the *Brachypodium distachyon* *TBL29* ortholog, together. Once created, the new sequence went through a digestion-ligation reaction with the BsaI/ccdB based expression vector, as both possessed cut sites for the BsaI restriction enzyme. This created a plasmid with the desired transgene that could be transformed into *Escherichia coli* to begin the bacterial transformation protocol (Carbonell et al., 2014). Sequences can be seen in Table 1.

Table 1: microRNA sequences used to knock down *TBL29* expression in *Brachypodium distachyon*

TBL29 microRNA Sequences	
Bradi1g65530 TBL29 amiRNA F1	CTTGTTGCGGGTGCGAAGCTTGCATATGATGATCA CATTTCGTTATCTATTTTTTTATGCAAGCTTAGCACCC GCAC
Bradi1g65530 TBL29 amiRNA R1	CATGGTGCGGGTGCTAAGCTTGCATAAAAAATAGA TAACGAATGTGATCATCATATGCAAGCTTCGCACC CGCAA
Bradi1g65530 TBL29 amiRNA F2	CTTGTACCCTAACCCTCCATTTCTAATGATGATCAC ATTTCGTTATCTATTTTTTTTAGAAATGGATGGTTAGG GTC
Bradi1g65530 TBL29 amiRNA R2	CATGGACCCTAACCATCCATTTCTAAAAAATAGA TAACGAATGTGATCATCATTAGAAATGGAGGGTTA GGGTA

CRISPR Construct Design – Both CRISPR constructs were designed to target multiple areas on the desired target gene or genes. For the *TBL29* CRISPR, two areas on *TBL29* were targeted (Figure 5, sequences in Table 2), and for the triple CRISPR, one area per gene (adding

up to three total areas) was targeted (Figures 5-7, sequences in Table 2, but the triple CRISPR only used the first gRNA for TBL29). The guide RNA sequences were selected from the online generator CRISPR-PLANT (Xie et al., 2014). This generator allowed for the selection of guide RNA sequences in the first exon, allowing for CRISPR/Cas9-mediated truncation of the amino acid sequence to occur before any functional domains are formed, creating the best possible chance for a non-functional protein. A published protocol was used in the CRISPR construct design (Xie et al., 2015). This protocol was selected because it allows for the CRISPR knockout of multiple genes at once, rather than crossing multiple single-CRISPR-knockout transformed lines (which is quite difficult in *Brachypodium distachyon*). This multiplex CRISPR activity is achieved by constructing a polycistronic gene able to produce multiple tRNAs and guide RNAs within the gene by taking over plant cells' tRNA processing systems. This protocol has also been linked with increased frequency of multiple simultaneous Cas9-mediated gene knockouts from a single transgene (Xie et al., 2015).

Table 2: CRISPR sequences used to knock out *TBL29*, *TBL34*, and *TBL35* expression in *Brachypodium distachyon*

CRISPR Constructs For <i>TBL29</i> , <i>TBL34</i> , and <i>TBL35</i>	
TBL29 Bradi1g65530 gRNA1 CRISPR F	GGCGGCCGTAAGTTTCTT
TBL29 Bradi1g65530 gRNA1 CRISPR R	GATGTCCTCGTTGTACAGGAAC
TBL29 Bradi1g65530 gRNA2 CRISPR F	GGTGTACGACGAGGTGAAC
TBL29 Bradi1g65530 gRNA2 CRISPR R	CCATTCCGCCTCCCTTTC
TBL34 Bradi4g44860 gRNA1 CRISPR F	TACTACTGATGGCCTGTCTCA
TBL34 Bradi4g44860 gRNA1 CRISPR R	AGTTGCACTCCTCCTCCT
TBL35 Bradi1g03970 gRNA1 CRISPR F	ATGTCGTCCGGGCGTTG
TBL35 Bradi1g03970 gRNA1 CRISPR R	GTTAGTATTACGATCATGGATGCTTGG

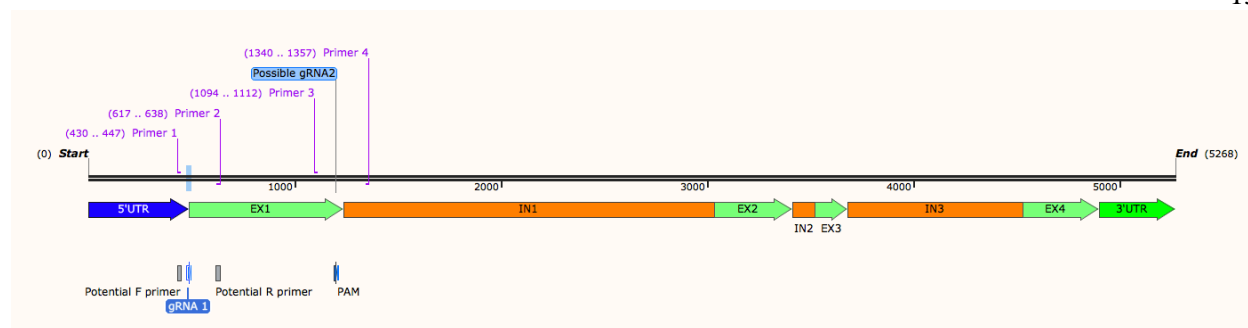


Figure 5: Schematic of *BdTBL29* gene showing the positions of both guideRNAs (gRNA 1 and Possible gRNA2) used for CRISPR construct design, as well as positions of primers (1-4) used for genotyping and sequencing.

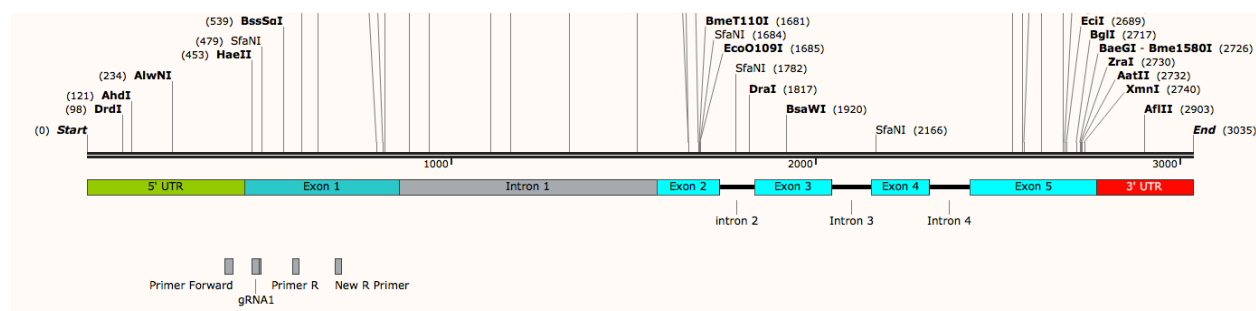


Figure 6: Schematic of *BdTBL34* gene showing the positions of the guideRNA (gRNA1) used for CRISPR construct design, as well as positions of primers (Primer Forward and New R Primer) used for genotyping and sequencing. Primer R was initially designed for genotyping, but did not work well.

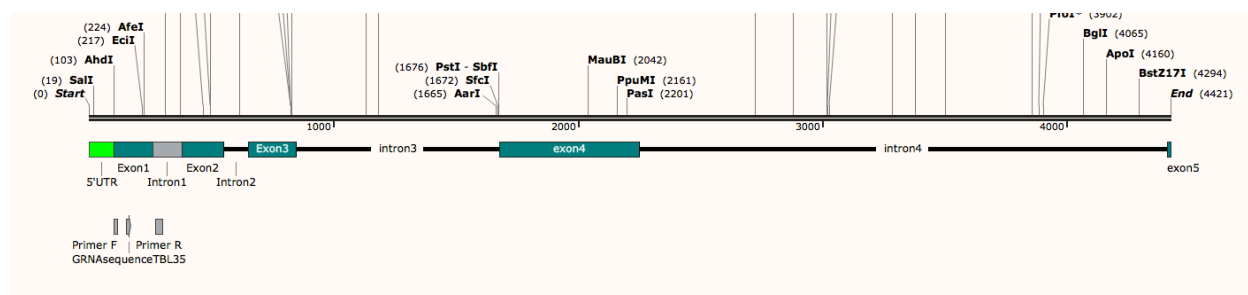


Figure 7: Schematic of *BdTBL35* gene showing the positions of the guideRNA (GRNasequenceTBL35) used for CRISPR construct design, as well as positions of primers (Primer F and Primer R) used for genotyping and sequencing.

Preparation of Callus – Embryos were removed from wild type *Brachypodium distachyon* (from the inbred line Bd 21-3) seeds. Before dissection, the each seed had its lemma removed, was incubated in sterilization solution (10% bleach and 0.1% Triton X-100 [Fisher, BP151-100])

for four minutes, and was washed with sterile water three times. Dissection involved carefully removing the embryo from the seed using very thin forceps and a dissecting microscope.

Embryos were placed onto callus induction media (CIM: 4.73 g/L Linsmaier and Skoog salts [Caisson Labs, LSP03-50LT], 30 g/L sucrose, pH 5.8, 2.5 g/L phytigel [Sigma-Aldrich, P8169-1KG]) containing 2.5 µg/mL 2,4 Dichlorophenoxyacetic acid (2,4 D) [Sigma, D7299-100G], a synthetic auxin that encourages growth. The embryos were incubated for 2-4 weeks in the dark at 28 degrees Celsius and the callus induction media was changed weekly (Vogel and Hill, 2007).

Transformation Protocol – Two days prior to the transformation, *Agrobacterium tumefaciens* strain AGL1 was smeared onto a plate containing MG media (5 g/L tryptone (Fischer-BP1421-500), 2.5 g/L yeast extract [Fisher-BP1422-500], 5 g/L sodium chloride, 5 g/L D-mannitol [Sigma, M1902-500G], 0.205 g/L magnesium sulfate heptahydrate [Fisher, BP213-1], 0.25 g/L potassium phosphate dibasic anhydrous [Fisher, P288-500], 1.2 g/L L-glutamic acid [Sigma-Aldrich, G5667-100G], pH 7.2). The two day incubation at 28 degrees Celsius allowed a lawn of *Agrobacterium* to form. The *Agrobacterium* lawn was then resuspended in liquid CIM, and its optical density at 600 nm was measured. After diluting the agrobacterium-liquid CIM solution so that its optical density was 0.6, 20 µL of acetosyringone [Sigma, D134406-5G] and 200 µL of Pluronic F68 detergent [Caisson Labs, PFL01-100ML] were added, completing the inoculation solution. At this point, the callus was added to the inoculation media. One plate of *Agrobacterium* makes enough inoculation solution for 10-12 plates of callus. After 5 minutes, the callus was removed and allowed to dry in the dark for three days, at 22 degrees Celsius (Vogel and Hill, 2007).

The callus, now exposed to the desired *TBL29* miRNA construct, *TBL29* CRISPR/Cas9 construct, or *TBL29/34/35* CRISPR/Cas9 construct, all of which contain a marker gene for hygromycin resistance, was then moved onto a new type of callus induction media (4.73 g/L Linsmaier and Skoog salts, 30 g/L sucrose, pH 5.8, 2.5 µg/mL 2,4 D) for three weeks. The media contained 40 µg/mL each of hygromycin [DOT Scientific, DSH75020-1], to kill any plant material that did not contain the transgene (Gritz and Davies, 1983), and timentin [Caisson Labs, T034-100GM], to kill the *Agrobacterium* after its delivery of the transgene (Nauerby et al., 1997). The callus was then grown on regeneration medium (4.73 g/L Linsmaier and Skoog salts, 30 g/L maltose, pH 5.8, 40 µg/mL hygromycin, 150 µg/mL timentin, 0.2 µg/mL kinetin [Caisson Labs, K001-1GM], 2.5 g/L phytigel), encouraging shoot development, for three more weeks. Kinetin was the key ingredient for shoot development, as it is a cytokinin hormone and increases cell division in the callus (Miller et al., 1955).

Growth of T₀ Generation – After shoots became evident on the regeneration medium, they were transplanted into magenta boxes containing rooting medium (4.42 g/L Murashige and Skoog salts + vitamins [Caisson Labs, MSP09-50LT], 30 g/L sucrose, pH 5.7, 0.2 µg/mL of the rooting hormone 1-Naphthaleneacetic acid, NAA [Caisson Labs, NSL01-100ML]). NAA has been shown to increase rooting in potentially stunted or auxin resistant mutant lines (Yamamoto and Yamamoto, 1998). Regenerants were grown in cycles of 16 hours of light, followed by 8 hours of darkness, for two weeks before being planted in soil made up of an equal mix of MetroMix 360 and MetroMix 510 soil. Height measurements were taken on a weekly basis. Plants were watered every two to three days and fertilized once to twice per week with Peter's Excel fertilizer [Griffin Greenhouse, 67-2306], depending on whether any potential nutrient deficiencies were spotted.

Growth of Subsequent Generations – After flowering and senescence of the T₀ generation, seeds were harvested from each plant. Ten seeds from each plant then had their lemma peeled off before being sterilized (10% bleach, 0.1% Triton X-100 solution) for ten minutes and washed three times with sterile water. The seeds were then transferred onto plates (1/4 MS, 1% sucrose, pH 5.6, 40 µg/mL hygromycin, 2.5 g/L phytigel) and stored in darkness at 4 degrees Celsius for 3 days and incubated at 22 degrees Celsius for 4 days under 24 hour light, before root lengths were measured and the new generation was planted, in soil as above. Any plants that had dead roots were classified as hygromycin sensitive, and were discarded, as they may not have taken up the desired transgene.

DNA Extraction – The Extract-N-Amp kit [Sigma-Aldrich, XNAP-1KT] protocol was followed for DNA extraction. A leaf snip of approximately 1-2 cm was taken from the selected plants and incubated at 95 degrees Celsius with 100 µL of extraction solution. After the incubation, 100 µL of dilution solution was added to each sample before storage at 4 degrees Celsius. DNA was then amplified via PCR using the Extract-N-Amp master mix, before being gel extracted and purified using the protocols from the same kit.

DNA Sequencing – Once pure DNA was extracted, 5 µL of each sample was taken and sent with 5 µL of 1mM primers (both forward and reverse) to the DNAlims facility at Pennsylvania State University for sequencing. Upon data return, sequences were compared to known wild-type DNA sequences for the genes of interest and any mutations were noted.

Chapter 3

***TBL29* microRNA Plants Do Not Show Significant Stunting Compared To Control Plants**

Transformant plants containing the *TBL29* microRNA construct were grown alongside seed containing a microRNA construct designed to knock down *GFP* expression to observe whether *TBL29* knockdown *Brachypodium* plants expressed phenotypes similar to those expressed in *TBL29* knockdown *Arabidopsis* plants. To observe this, height measurements were taken for the *TBL29* microRNA T1 generation and compared to the heights of the *GFP* microRNA T1 generation (Figure 8).

***TBL29* microRNA T1 Height Measurements Show No Significant Stunting Compared To *GFP* microRNA T1 Height Measurements**

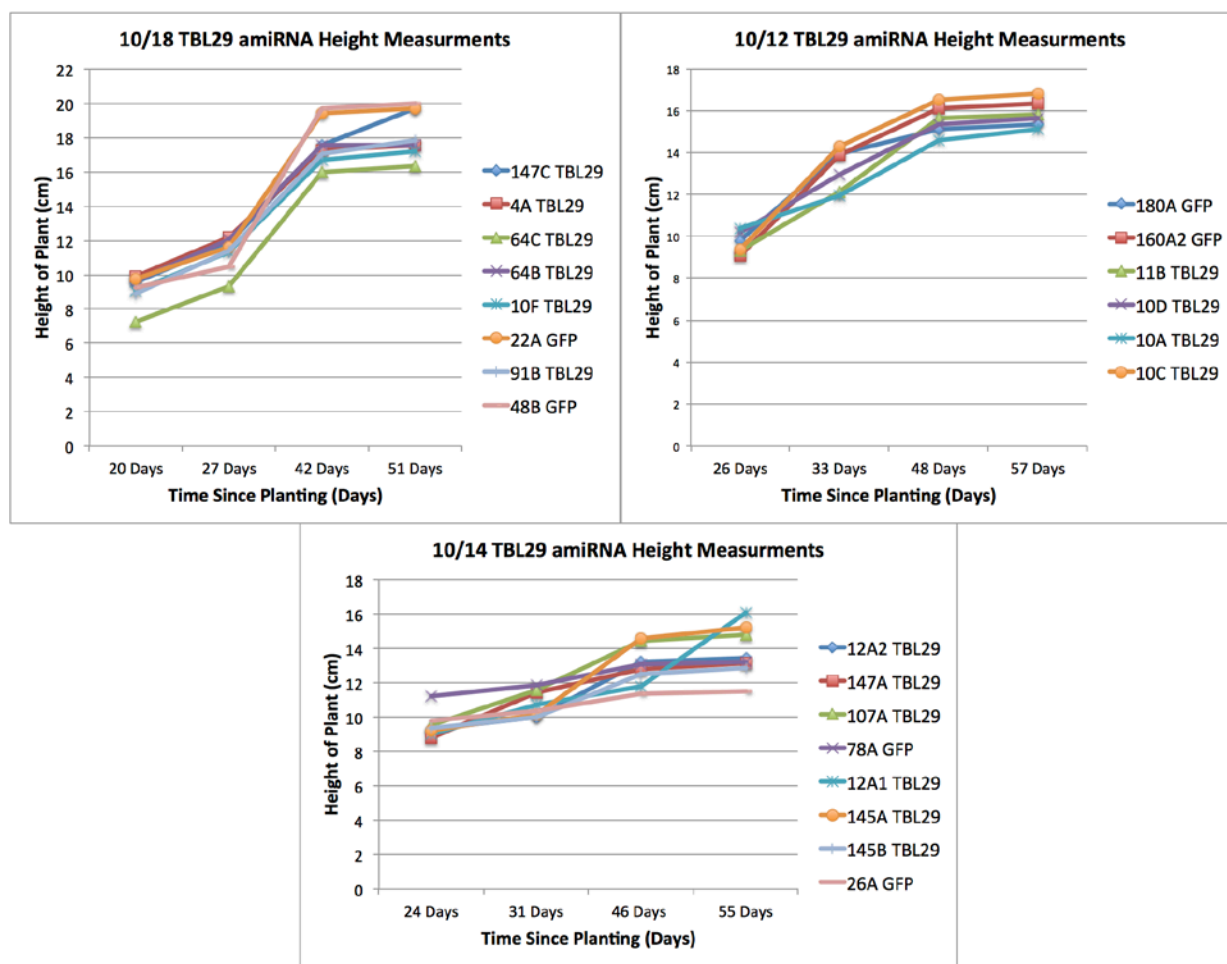


Figure 8: *TBL29* amiRNA Height Data. Most of the TBL lines contained between 8 and 10 plants (lines 64B and 64C only had four surviving seed from the T0 generation). These plants were compared to *GFP* amiRNA lines containing between 8 and 12 plants per sample. No significant differences between plant heights were detected ($p > 0.05$, T-test).

The growth patterns of the T1 generation of *TBL29* and *GFP* microRNA lines were charted (Figure 8). Due to the volume of lines that survived the throughout the T0 generation and produced seed, three separate plantings were necessary. The lines from the three plantings were kept in the same growth chamber, ensuring that they had the same watering schedule (every 2-3 days) and light/dark schedule (16 hours of light followed by 8 hours of dark). The lack of

significant height differences between the *TBL29* microRNA lines and the *GFP* microRNA lines led to further experimentation on whether complete knockout of *TBL29* with CRISPR/Cas9 gene editing methods would lead to increased instances of stunting in transgenic mutants, as shown in *Arabidopsis* and *Oryza* (Yuan et al., 2016 and Gao et al., 2017).

Chapter 4

***TBL29* CRISPR Plants Show Some Significant Stunting Compared To *GFP* CRISPR Plants**

Transformant plants containing the *TBL29* CRISPR/Cas9 gene construct were grown alongside transformant plants containing the *GFP* CRISPR/Cas9 gene construct. The *TBL29* CRISPR lines were expected to show stunted growth because of the nature of the CRISPR construct: designed to cause mutations in the first exon of *TBL29*. Any frameshift mutations that occurred that early in the amino acid sequence would likely lead to a severely truncated, non-functional protein. This experiment was prepared to observe whether *TBL29* knockouts expressed phenotypic effects in *Brachypodium* similar to those expressed in *Arabidopsis*. To observe this, height measurements were taken for the *TBL29* CRISPR T1 generation and compared to the heights of the *GFP* CRISPR T1 generation (Figure 9).

***TBL29* CRISPR T1 Height Data Shows Some Significant Stunting Compared To *GFP* CRISPR T1 Height Data**

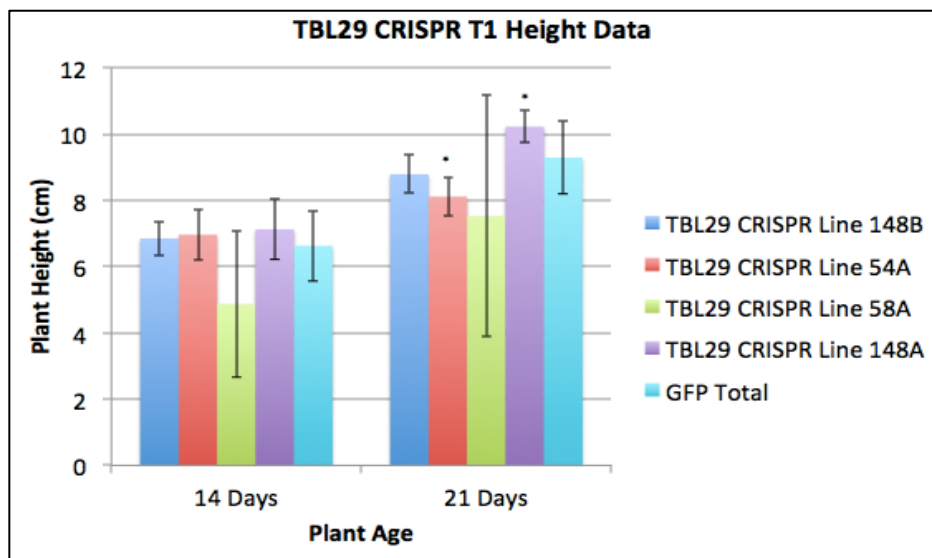


Figure 9: TBL29 CRISPR Height Data. The four surviving CRISPR lines (ten plants each) were compared to two GFP CRISPR lines (total of 11 plants). Error bars represent standard deviation. Asterisks (*) indicate significant difference from the GFP control (p<0.05, T-test).

From the T0 generation, only four plants survived and produced enough seed for planting a new generation. The four transformants (transformant 148B, transformant 54A, transformant 58A, and transformant 148A) were grown on MS plates containing hygromycin along with two lines of GFP CRISPR T0 seed (line 27A and line 68A). The GFP CRISPR lines were combined into one group (the GFP group on the above chart) when being compared to the knockout lines. These data came closer to replicating previous data on stunting prevalence in *Arabidopsis* plants with knocked out *TBL29* genes than the microRNA experiments had. Additionally, they led to the question of whether knocking out multiple xylan acetylation genes would have an even stronger phenotype, similar to what was shown in *Arabidopsis* (Yuan et al., 2016). Despite this, there was one line (line 148A) that was consistently taller than the control plants. This does not fit in with the data from the previous studies, but will be an interesting line to monitor in future generations.

Chapter 5

***TBL29/34/35* CRISPR Plants Show Some Stunting, As Well As Increased Lethality And Drought Stress Symptoms, Compared To *GFP* CRISPR Plants**

Transformant plants containing the *TBL29*, *TBL34*, and *TBL35* CRISPR/Cas9 gene constructs were grown alongside transformant plants containing the *GFP* CRISPR/Cas9 gene construct. The *TBL29/34/35* CRISPR lines were expected to show stunted growth because of the nature of the CRISPR construct: designed to cause mutations in the first exons of *TBL29*, *TBL34*, and *TBL35*. Any frameshift mutations that occurred that early in the amino acid sequence would likely lead to severely truncated, non-functional proteins. This experiment's purpose was to observe whether *TBL29/34/35* knockouts expressed phenotypic effects in *Brachypodium* similar to those expressed in *Arabidopsis*. To observe this, the survival rates of the T0 generations of *TBL29/34/35* CRISPR plants (Table 3) and *GFP* CRISPR plants (Table 4) were charted. This was to determine whether the *TBL29/34/35* CRISPR transgene showed a lethality phenotype. Additionally, height measurements were taken for the *TBL29/34/35* CRISPR T1 generation and compared to the heights of the *GFP* CRISPR T1 generation (Figure 10). Tissue samples (leaf snips) were taken from visibly stunted *TBL29/34/35* CRISPR lines. These samples underwent DNA extraction, and were sequenced, along with *GFP* CRISPR lines, to determine whether mutations in the *TBL* genes of interest correlated with stunted growth (Table 5). Photos were taken of plants from the *TBL29/34/35* CRISPR T1 generation and the *GFP* CRISPR T1 generation to show whether stunting and drought stress syndrome phenotypes, such as xylem collapse, were visible (Figures 11-13).

T0 Generation Survivability Results Show Increased Lethality In *TBL29/34/35* CRISPR Plants, When Compared To *GFP* CRISPR Plants

Table 3: *TBL29/34/35* CRISPR T0 Generation Results. This table shows the fate of each of the *TBL29/34/35* CRISPR lines that survived through tissue culture and were planted. Each transformant was assigned a number for survivability, with 0 meaning that the transformant died, 0.5 meaning that the transformant lived, but produced no usable seed, and 1 meaning that the transformant lived and produced seed.

TBL 29/34/35 CRISPR T0 Generation Results		
CRISPR Line	Result	Survivability
140A	Died	0
20B	Died	0
166A	Died	0
140B	Died	0
49A	Died	0
60A	Died	0
19A	Died	0
132A	Died	0
130A	Lived, but no usable seed produced	0.5
18B	Died	0
62A	Lived	1
131A	Died	0
136A	Lived	1
161A	Lived	1
3A	Died	0

Table 4: *GFP* CRISPR T0 Generation Results. This table shows the fate of each of the *GFP* CRISPR control lines that survived through tissue culture and were planted. Survivability scale is the same as the scale used in Table 3.

<i>GFP</i> CRISPR T0 Generation Results		
CRISPR Line	Result	Survivability
111A	Died	0
31A	Lived	1
5A	Lived	1
1A	Lived	1
31B	Died	0
104A	Lived	1
1B	Lived	1
31C	Died	0
27A1	Lived	1

These tables show the survival rates of both the *TBL29/34/35* Triple CRISPR T0 generation (Table 3) and the *GFP* CRISPR T0 generation (Table 4). During tissue culture each of the transformants was moved from regeneration media to MS media and stored for two weeks at 28 degrees Celsius. They were then moved to soil, where they were watered every two to three days and fertilized once to twice per week. It was initially hypothesized that the rigorous nature of the transformation process led to the high death rates in the *TBL29/34/35* CRISPR T0 plants. However, the *GFP* CRISPR T0 plants had significantly lower death rates, leading to thoughts that knocking out multiple xylan acetylation genes could have a degree of lethality in transformant lines. This significance was obtained by assigning a “survivability value” to each of the transformants. Transformants that survived received a “1,” transformants that died received a “0,” and the one transformant that survived, but failed to produce usable seed received a “0.5.” The fact that many more *TBL29/34/35* CRISPR T0 plants than *GFP* CRISPR T0 plants died led to a hypothesis that the *TBL29/34/35* CRISPR T1 generation of transformants would exhibit severe stunting, similar to previous studies on *Arabidopsis* (Gao et al., 2017).

T1 Height Data Shows Some Stunting In *TBL29/34/35* CRISPR Lines Compared To *GFP* CRISPR Lines

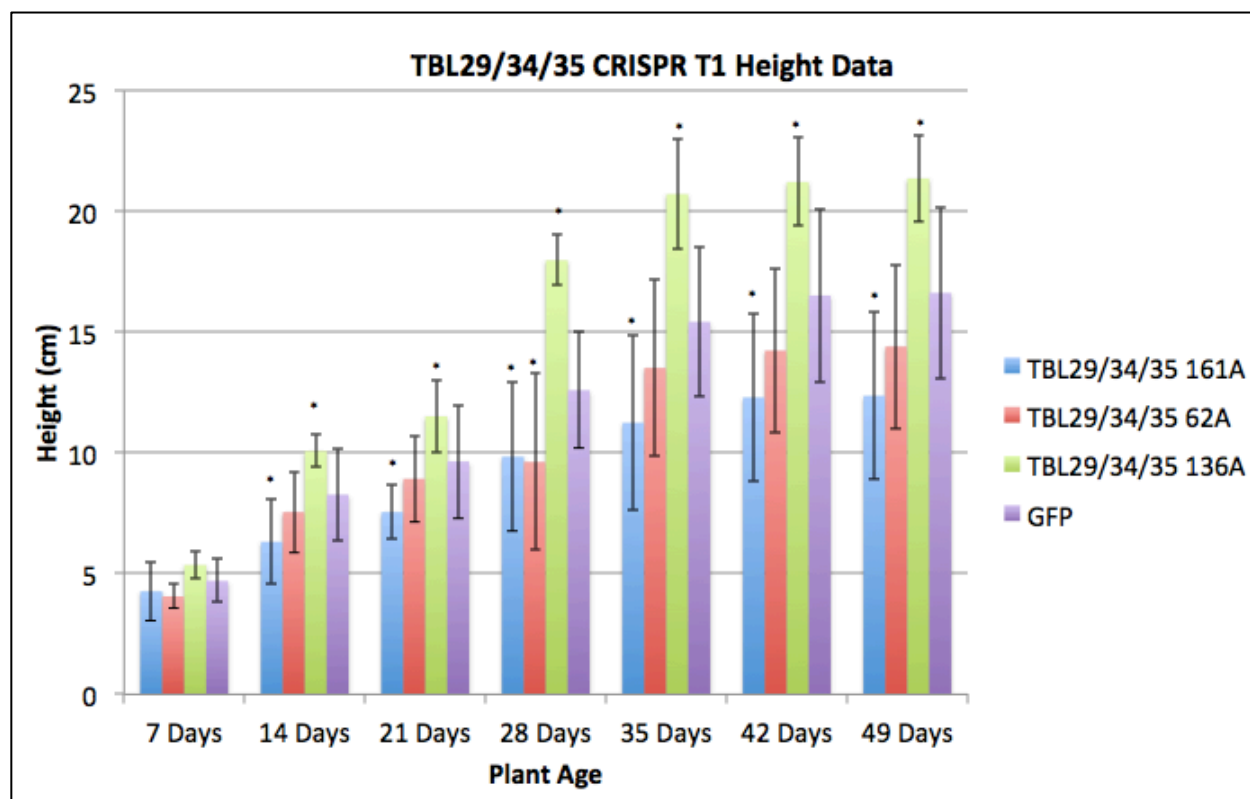


Figure 10 *TBL29/34/35* Triple CRISPR Height Data. The three surviving triple CRISPR lines (ten plants each) were compared to two *GFP* CRISPR lines (total of 11 plants). Error bars represent standard deviation. Asterisks (*) indicate significant difference from the *GFP* control ($p < 0.05$, T-test).

From the T0 generation, only three plants survived and produced enough seed for planting a new generation (Table 3). The three lines (line 161A, line 62A, and line 136A) were grown on hygromycin plates with two lines of *GFP* CRISPR T0 seed (line 1A and line 5A). The *GFP* CRISPR lines were combined into one group (the *GFP* group on the above chart) when being compared to the knockout lines. The degree of stunting in the triple CRISPR T1 lines was similar to that of the single CRISPR T1 lines, with only one significantly stunted line in each

group, as well as one line that was significantly larger than the control lines. This does not match conclusions from previous studies (Gao et al., 2017), but the T1 generation may be too early to observe line-wide stunted growth. The Stunted individuals that did emerge from these lines had leaf samples (1-2 cm of leaf tissue total) taken for DNA sequence analysis.

Sequencing Data Shows The Correlation Between Mutations In *TBL29*, *34*, and *35* And Stunted Growth

Table 5: Sequencing data for stunted *TBL29/34/35* Triple CRISPR plants and *GFP* control. The plants were each identified by their line and plant number, as well as what the sequencing data showed at each locus of interest.

<i>TBL29/34/35</i> CRISPR T1 Stunted Individuals			
Plant	<i>TBL29</i>	<i>TBL34</i>	<i>TBL35</i>
161A.1	Frameshift	Frameshift	Frameshift
161A.2	Frameshift	No Mutation	Frameshift
161A.3	Frameshift	No Mutation	Too Many Ns
161A.4	Frameshift	No Mutation	Frameshift
161A.5	Frameshift	No Mutation	Frameshift
161A.8	Frameshift	No Mutation	Frameshift
62A.1	Frameshift	Frameshift	Frameshift
62A.4	Frameshift	Frameshift	No Mutation
<i>GFP</i> 5A.9	Inconclusive	No Mutation	Inconclusive

This table shows the sequencing data from each of the 8 severely stunted plants from the T1 generation compared to the wild type DNA gathered from Phytozome (Goodstein et al, 2011). Frameshift mutations indicate a nonfunctional gene, due to the fact that the codon sequence was disrupted completely. “No mutation,” indicates that the sequencing data matched the wild type sequence. “Inconclusive,” and “too many Ns” indicate that the sequencing data was not strong enough to accurately analyze. This can be caused by a dilute sample, leading to a lack of strong peaks in the sequencing data. The correlation between frameshift mutations and

stunted the stunted nature of these plants supports the hypothesis that knocking out multiple xylan acetylation genes causes stunted growth. Additionally, the lack of transformants with frameshift mutations across all three xylan acetylation genes brings forth the possibility that, in *Brachypodium*, knocking out all three xylan acetylation genes leads to decreased survivability among transformants.

Structural Comparison Shows Drought Stress Symptoms In *TBL29/34/35* CRISPR Plants But Not *GFP* CRISPR Plants

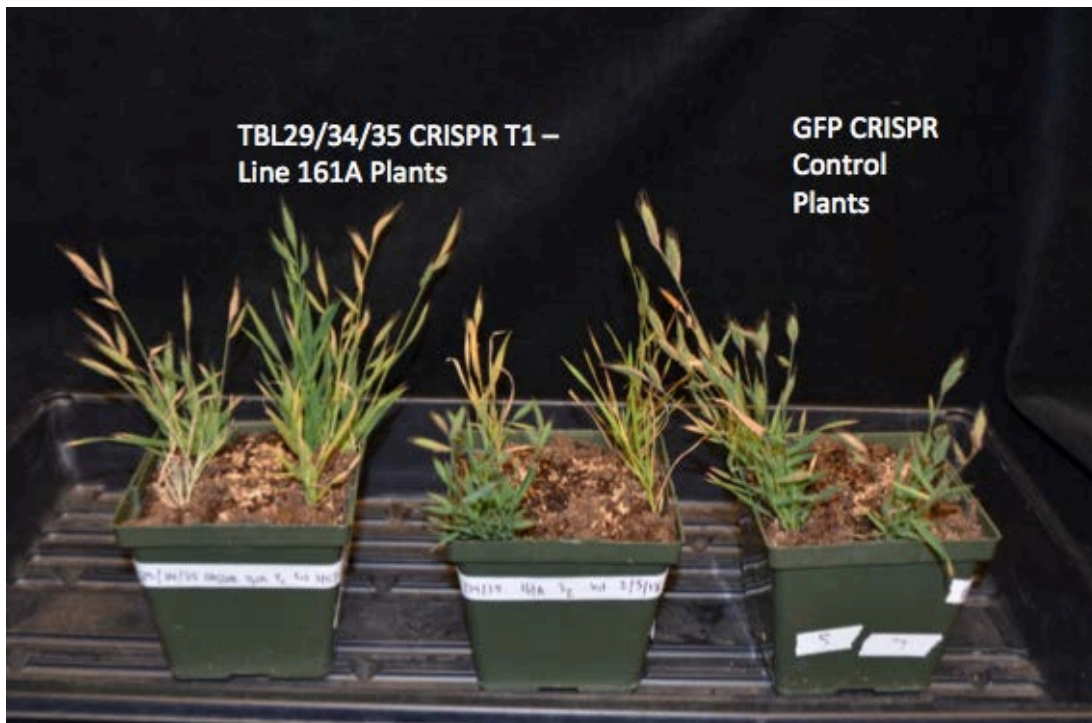


Figure 11: Two pots of *TBL29/34/35* CRISPR T1 line 161A plants compared to plants from the *GFP* control.



Figure 12: Photograph of stem of plant number 2 from *TBL29/34/35* CRISPR line 161A showing stunting and drought-like phenotypes. A large number of leaves and stems from this line were thinner and showed different coloration than both *GFP* CRISPR controls and other *TBL29/34/35* CRISPR lines.



Figure 13: Photograph of stem from plant number 6 of *GFP* CRISPR Control. This stem represents the non-stunted, non-drought phenotype.

Side by side comparisons of *TBL29/34/35* CRISPR lines and *GFP* CRISPR lines (Figure 11) show the stunted nature of knockout lines in comparison to control. Certain individuals in line 161A showed physical signs of collapsed xylem in addition to their stunting. These data support the hypothesis that knocking out multiple genes responsible for xylan acetylation causes drought stress symptoms in *Brachypodium*, just as it does in *Arabidopsis* (Bensussan et al., 2015). While stem sections have not been made yet, the lack of structural support in *TBL29/34/35* CRISPR line 161A.2 (Figure 12) compared to *GFP* CRISPR line 5A.6 (Figure 13) hints toward the presence of collapsed xylem. Another symptom of collapsed xylem is decreased seed production (Bensussan et al., 2015). *TBL29/34/35* CRISPR line 161A.2 (Figure 12) has only one visible seed spikelet on its inflorescence, while *GFP* CRISPR line 5A.6 (Figure 13) has four. The seed spikelets from *GFP* CRISPR line 5A.6 also show more seed fill than their counterpart from *TBL29/34/35* CRISPR line 161A.2. Both of these factors support the hypothesis that knocking out multiple genes responsible for xylan acetylation causes drought stress symptoms.

Chapter 6

Discussion

The *TBL29* microRNA lines showed no significant differences from *GFP* lines in terms of plant height (figure 8). It will be difficult to determine whether any of these lines had expressed the microRNA or which lines expressed it most until Quantitative Polymerase Chain Reaction (qPCR) is performed. The qPCR will allow for the measurement of overall *TBL29* expression in each of the selected *TBL29* microRNA T1 plants. This will be accomplished by extracting RNA from each of the selected plants and using Reverse Transcriptase Polymerase Chain Reaction (RT PCR) to create complementary DNA (cDNA, DNA generated from single-stranded RNA) for the qPCR reaction. Figure 14 refers to the expression map for *TBL29*, which shows that the *TBL29* gene is expressed at the highest levels in the stem, specifically the second internode and the peduncle. As a result of this, second internode and peduncle tissue were taken from 80 total plants across the T1 generation (with at least 2 samples from every surviving line) and frozen at negative eighty degrees Celsius for future RT PCR and qPCR analysis.

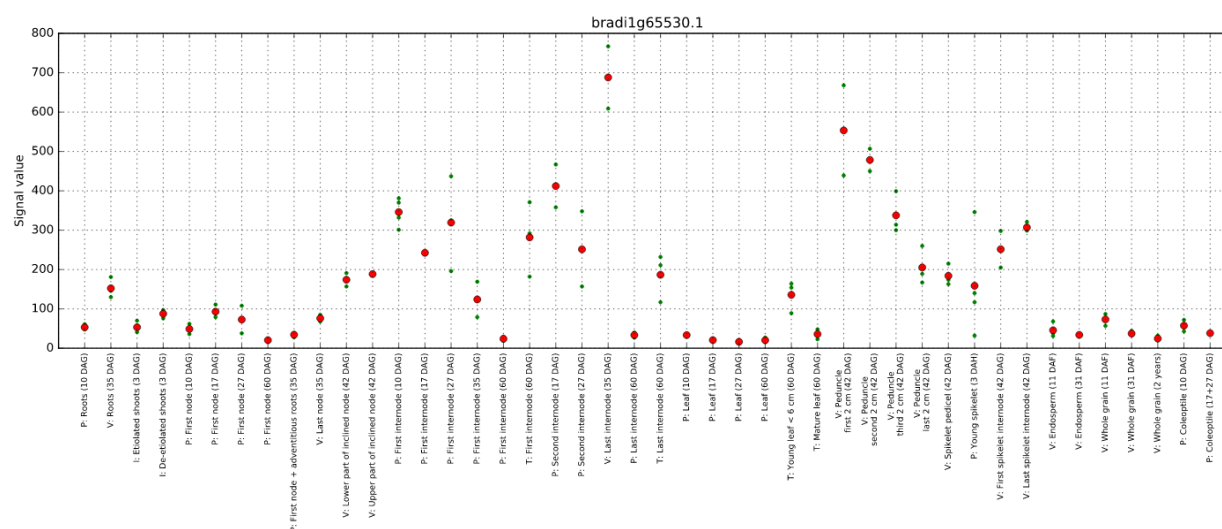


Figure 14: Expression profile of TBL29, showing which parts of the plant anatomy express TBL29 at the highest levels. (Petrik, 2018)

The *TBL29* CRISPR T1 height data (Figure 9) was similar to the triple CRISPR height data (figure 10). Both data sets had one line that was significantly taller than the *GFP* control group and one line that was significantly shorter than the *GFP* control group. For the *TBL29* T1 plants, line 148A was significantly taller than the control group, while line 54A showed significant stunting compared to the control group. This generation is still in the process of growing, so there are fewer data points than the triple CRISPR data. Despite this, the limited amount of data gathered can be trusted, because, in the triple CRISPR lines, significance first began to emerge around the 14 to 21 days after planting. Additionally, it should be noted that line 58A had the lowest average height among all of the *TBL29* CRISPR lines, but its rather large standard deviation prevents it from being considered significant. This is due to the fact that the line seems to be split between severely stunted plants and plants growing at a normal rate. As for line 148A, it is possible that CRISPR/Cas9 mutations were less severe (addition or deletion of an amount of bases equal to a multiple of three) for all ten of the seed in the line. Ten seeds is a relatively small sample size, so the T2 generation of line 148A will be instrumental in

determining whether this phenotype is significant or an aberration. This is true for all of the *TBL29* CRISPR T1 data. It is possible that the T1 generation is too early to check for significant stunting effects for this transgene. This is due to the fact that finding a fully homozygous expression of the transgene may not be possible until the T2 generation, as fully homozygous seed do not emerge until the T1 generation, and a line composed entirely of such seed would be possible in the T2 generation at the earliest. This is significant because it is possible that one wild type allele for *TBL29* could cause the acetyltransferase to remain operational within the organism.

The *TBL29/34/35* Triple CRISPR data for the T0 generation (Table 3) shows that 11 out of 15 (73%) of triple CRISPR knockouts were stunted and died (additionally, one line, 130A, grew to a normal height, but failed to produce viable seed). This could be attributed the stresses of bacterial transformation and having to grow on media for weeks before being placed into soil. However, of the 9 *GFP* CRISPR lines (Table 4) that were transformed alongside of the *TBL29/34/35* Triple CRISPR lines, only 3 lines (33%) died, suggesting that transformation with the *TBL29/34/35* Triple CRISPR construct increased the mortality of the transformed plants.

The *TBL29/34/35* Triple CRISPR height data for the T1 generation shows that one of the lines (line 161A) showed significant stunting (Figure 10). Line 62A was also consistently shorter than the *GFP* CRISPR control lines, but the p value fluctuated, leading to a lack of consistent significance. Line 136A presented consistent significance, but the plants from the line were consistently significantly taller than the *GFP* CRISPR control lines. The lack of a group of consistently stunted lines may have been caused by the fact that the T1 generation was only made up of plants that produced seed in the T0 generation. A large portion of the T0 generation showed significant stunting, but most of those plants failed to live long enough to produce usable

seed. The plants that survived to produce seed were the tallest of the group, implying that their CRISPR mutations were not homozygous. The presence of a normal allele in the T0 seed allows for the possibility that the T1 generation contained three genotypes: homozygous for non-mutated DNA, which would likely be non-stunted, heterozygous, which would likely be non-stunted due to the presence of the one wild type allele for *TBL29* and homozygous for the CRISPR mutated DNA, which would likely be stunted. The expected phenotypic ratio would be 3:1 in favor of non-stunted. This leads to the possibility that, when choosing 10-12 seeds to plate for the next generation, nearly all of the selected seeds could be of the non-stunted variety.

The photos of the stunted line (line 161A) compared with the non-stunted *GFP* lines (Figure 11) support the hypothesis that some of the stunted 161A lines exhibit collapsed xylem. Drought stress is often an indicator of collapsed xylem (Lugan et al, 2009). The yellowed leaves on the stunted individuals from 161A are thought to be caused by drought stress. All of the plants in the study were fertilized twice per week, so a nutrient deficiency would be unlikely. Additionally, only stunted plants presented these symptoms. None of the non-stunted plants (presumably with functional xylem) showed any of the common symptoms of nutrient stress in the wheat family, such as leaf curling (nitrogen deficiency), chlorotic spotting (chlorine deficiency), yellow patches (magnesium deficiency), or light green or yellow leaves (sulfur or iron deficiencies, respectively) (McCauly et al., 2011).

The sequencing data for the *TBL29/34/35* Triple CRISPR T1 lines attempts to correlate more serious mutations, such as frameshift mutations in the three *TBL* genes, with stunting (Table 5). All of the stunted plants presented frameshift mutations in the *TBL29* gene, while 6 of the 8 stunted plants also showed frameshift mutations in *TBL35* and only 3 of the 8 plants showed frameshift mutations in *TBL34*. The two plants that had no frameshift in *TBL35* (161A.3

and 62A.4) either had a frameshift mutation in *TBL34* (62A.4) or exhibited an inconclusive sequence (161A.3). These data could imply that inactivation across all three *TBL* genes causes a higher instance of lethality in *Brachypodium distachyon*, as most of the stunted lines (6 out of the 8) still had at least one active *TBL* gene (usually *TBL34*). That being said, the sample size is quite small (n=8), so more will be known after the T2 generation.

The next steps in the process are a biochemical analysis of the *TBL29* and *TBL29/34/35* CRISPR lines, as well as immunolabeling and imaging transgenic plant material. The biochemical analysis includes an assay to test the levels of acetylation of the stunted CRISPR plants compared to control plants and non-stunted CRISPR plants. The protocol is adapted from an acetyl esterase activity assay, and involves generating alcohol insoluble residue (AIR) and using acid alcohol solution to remove the acetyl groups from xylan. The optical density can then be measured via spectrophotometer to quantify the amount of acetyl residues removed from the collected plant material (Pogorelko, 2014). This method has already been successfully used on tissue from both *Arabidopsis thaliana* and *Brachypodium distachyon* (Pogorelko 2013). Another way that levels of acetylation can be view is with immunolabeling using the LM28 antibody (Cornuault et al., 2015). This provides a more indirect gauge into the acetylation levels of the transgenic lines. The LM28 antibody actually binds to glucuronic acid residues rather than acetyl residues, but there is evidence that reducing xylan acetylation can lead to an increase in methylglucuronic acid prevalence in xylan (Grantham et al., 2017). Therefore, it is expected that the stunted transgenic plants will show the most fluorescence when analyzed in this matter. Additionally, to further test the hypothesis that the triple CRISPR line 161A's stunting includes collapsed xylan, stem sections will be made an stained with toluidine blue dye. This will allow

the xylem vessels to be viewed and compared to CRISPR non-stunted plants and *GFP* CRISPR control plants (O'Brien, 1964).

Chapter 7

Conclusion

This research has made significant strides towards answering the proposed questions. A large portion of this project was composed of set-up for the projects, as well as for future projects: microRNA and CRISPR construct design, transformation, and growth of early generations. The early returns are promising. Stunted growth and drought stress symptoms are visible in a subset of the T1 generations in both groups of CRISPR/Cas9 transformants. Future biochemical assays and imaging will supplement this data further, while the planting of future generations will allow for lines of plants homozygous for the frameshift mutation in *TBL29* or all three of the *TBL29*, *TBL34*, and *TBL35* genes to be studied further.

BIBLIOGRAPHY

1. Bensussan, M., Lefebvre, V., Ducamp, A., Trouverie, J., Gineau, E., Fortabat, MN., Guillebaux, A., Baldy, A., Naquin, D., Herbette, S., Lapierre, C., Mouille, G., Horlow, C., Durand-Tardif, M. (2015). Suppression of Dwarf and irregular xylem Phenotypes Generates Low-Acetylated Biomass Lines in Arabidopsis. *Plant Physiology*, 168(2), 452-463. doi:10.1104/pp.15.00122
2. Bromley, J. R., Busse-Wicher, M., Tryfona, T., Mortimer, J. C., Zhang, Z., Brown, D. M., Dupree, P. (2013) GUX1 and GUX2 glucuronosyltransferases decorate distinct domains of glucuronoxytan with different substitution patterns. *The Plant Journal*, 74(3), 423-434. doi: 10.1111/tpj.12135
3. Brown, D. M., Goubet, F., Wong, V. W., Goodacre, R., Stephens, E., Dupree, P., & Turner, S. R. (2007). Comparison of five xylan synthesis mutants reveals new insight into the mechanisms of xylan synthesis. *The Plant Journal*, 52(6), 1154-1168. doi:10.1111/j.1365-313x.2007.03307.x
4. Caballero, B., Trugo, L. C., & Finglas, P. M. (2003). *Encyclopedia of food sciences and nutrition*. Amsterdam: Academic press.
Entry by M.T. Holtzapple on hemicelluloses, pgs 3060-3071
5. Carbonell, A., Takeda, A., Fahlgren, N., Johnson, S. C., Cuperus, J. T., & Carrington, J. C. (2014). New Generation of Artificial MicroRNA and Synthetic Trans-Acting Small Interfering RNA Vectors for Efficient Gene Silencing in Arabidopsis. *Plant Physiology*, 165(1), 15-29. doi:10.1104/pp.113.234989
6. Carroll A., Somerville C. (2009) Cellulosic biofuels. *Annu Rev Plant Biol* 60: 165-182
7. Cass CL., Peraldi A., Dowd PF., Mottiar Y., Santoro N., Karlen SD., Bukhman YV., Foster CE., Thrower N., Bruno LC., Moskvina OV., Johnson ET., Willhoit ME., Phutane M., Ralph J., Mansfield SD., Nicholson P., Sedbrook JC. (2015) Effects of PHENYLALANINE AMMONIA LYASE (PAL) knockdown on cell wall composition, biomass digestibility, and biotic and abiotic stress responses in Brachypodium. *J Exp Bot* 66: 4317-4335
8. Cornuault, V., Buffet, F., Rydahl, M.G., Marcus, S.E., Torode, T.A., Xue, J., Crepeau, M.J., Faria-Blanc, N., Willats, W.G., Dupree, P., Ralet, M.C. and Knox, J.P. (2015) Monoclonal antibodies indicate low-abundance links between heteroxytan and other glycans of plant cell walls. *Planta*, 242(6), 1321-1334. doi:10.1007/s00425-015-2375-4
9. Cosgrove, D. J., & Jarvis, M. C. (2012). Comparative structure and biomechanics of plant primary and secondary cell walls. *Frontiers in Plant Science*, 3. doi:10.3389/fpls.2012.00204
10. El Refy, A., Perazza, D., Zekraoui, L., Valay, J., Bechtold, N., Brown, S., Hülskamp, M., Herzog, M., Bonneville, JM. (2003). The Arabidopsis KAKTUS gene encodes a HECT protein and controls the number of endoreduplication cycles. *Molecular Genetics and Genomics*, 270(5), 403-414. Retrieved April 6, 2018.
11. Eliasson, A. (2004). *Starch in food: Structure, function and applications*. Cambridge, England: Woodhead Pub.

12. Fahlgren, N, Hill ST, Carrington JC, Carbonell A (2016) P-SAMS: a web site for plant artificial microRNA and synthetic trans-acting small interfering RNA design. *Bioinformatics* 32: 157-158. doi: 10.1093/bioinformatics/btv534
13. Gao Y, He C, Zhang D, Liu X, Xu Z, Tian Y, Liu XH, Zang S, Pauly M, Zhou Y, Zhang B (2017) Two Trichome Birefringence-Like Proteins Mediate Xylan Acetylation, Which Is Essential for Leaf Blight Resistance in Rice. *Plant Physiol* 173: 470-481
14. Gille, S., Souza, A. D., Xiong, G., Benz, M., Cheng, K., Schultink, A., Reza, IB., Pauly, M. (2011). O-Acetylation of Arabidopsis Hemicellulose Xyloglucan Requires AXY4 or AXY4L, Proteins with a TBL and DUF231 Domain. *The Plant Cell*, 23(11), 4041-4053. doi:10.1105/tpc.111.091728
15. Goodstein, D. M., Shu, S., Howson, R., Neupane, R., Hayes, R. D., Fazo, J., Mitros, T., Dirks, W., Hellsten, U., Putnam, N., Rokhsar, D. S. (2011). Phytozome: A comparative platform for green plant genomics. *Nucleic Acids Research*, 40(D1). doi:10.1093/nar/gkr944
16. Grantham, N. J., Wurman-Rodrich, J., Terrett, O. M., Lyczakowski, J. J., Stott, K., Iuga, D., Simmons, TJ., Durand-Tardif, M., Brown, SP., Dupree, R., Busse-Wicher, M., Dupree, P. (2017). An even pattern of xylan substitution is critical for interaction with cellulose in plant cell walls. *Nature Plants*, 3(11), 859-865. doi:10.1038/s41477-017-0030-8
17. Gritz, L., & Davies, J. (1983). Plasmid-encoded hygromycin B resistance: The sequence of hygromycin B phosphotransferase gene and its expression in *Escherichia coli* and *Saccharomyces cerevisiae*. *Gene*, 25(2-3), 179-188. doi:10.1016/0378-1119(83)90223-8
18. He, L., & Hannon, G. J. (2004). Correction: MicroRNAs: Small RNAs with a big role in gene regulation. *Nature Reviews Genetics*, 5(8), 631-631. doi:10.1038/nrg1415
19. International Rice Genome Sequencing Project. (2005). *The map based sequence of the rice genome*.
20. Javeline, D., Hellmann, J. J., Mclachlan, J. S., Sax, D. F., Schwartz, M. W., & Cornejo, R. C. (2015). Expert opinion on extinction risk and climate change adaptation for biodiversity. *Elementa: Science of the Anthropocene*, 3, 000057. doi:10.12952/journal.elementa.000057
21. Lugan, R., Niogret, M., Kervazo, L., Larher, F. R., Kopka, J., & Bouchereau, A. (2009). Metabolome and water status phenotyping of Arabidopsis under abiotic stress cues reveals new insight into ESK1 function. *Plant, Cell & Environment*, 32(2), 95-108. doi:10.1111/j.1365-3040.2008.01898.x
22. Manabe, Y., Nafisi, M., Verhertbruggen, Y., Orfila, C., Gille, S., Rautengarten, C., Cherk, C., Marcus, SE., Somerville, S., Pauly, M., Knox, JP., Sakuragi, Y., Scheller, H. V. (2011, March). Loss-of-function mutation of REDUCED WALL ACETYLATION2 in Arabidopsis leads to reduced cell wall acetylation and increased resistance to Botrytis cinerea. *Plant Physiology*, 155, 1068-1078
23. McCauly, A., Jones, C., & Jacobson, J. (2011). *Plant Nutrient Functions and Deficiency and Toxicity Symptoms* [Pamphlet].
24. Miller, C. O., Skoog, F., Saltza, M. H., & Strong, F. M. (1955). Kinetin, A Cell Division Factor From Deoxyribonucleic Acid1. *Journal of the American Chemical Society*, 77(5), 1392-1392. doi:10.1021/ja01610a105
25. Naik, S. N., Goud, V. V., Rout, P. K., & Dalai, A. K. (2010). Production of first and second generation biofuels: A comprehensive review. *Renewable and Sustainable Energy Reviews*, 14, 579-593

26. Nauerby, B., Billing, K., & Wyndaele, R. (1997). Influence of the antibiotic timentin on plant regeneration compared to carbenicillin and cefotaxime in concentrations suitable for elimination of *Agrobacterium tumefaciens*. *Plant Science*, 123(1-2), 169-177. doi:10.1016/s0168-9452(96)04569-4
27. Nigam, P. S., & Singh, A. (2011). Production of liquid biofuels from renewable resources. *Progress in Energy and Combustion Science*, 37(1), 52-68. doi:10.1016/j.pecs.2010.01.003
28. O'Brien, T. P., Feder, N., & McCully, M. E. (1964). Polychromatic staining of plant cell walls by toluidine blue O. *Protoplasma*, 59(2), 368-373. doi:10.1007/bf01248568
29. Pogorelko, G., Lionetti, V., Fursova, O., Sundaram, R. M., Qi, M., Whitham, S. A., Bogdanove, A.J., Bellincampi, D., Zabortina, O. A. (2013). Arabidopsis and Brachypodium distachyon Transgenic Plants Expressing *Aspergillus nidulans* Acetyltransferases Have Decreased Degree of Polysaccharide Acetylation and Increased Resistance to Pathogens. *Plant Physiology*, 162(1), 9-23. doi:10.1104/pp.113.214460
30. Pogorelko, G., & Zabortina, O. (2014). Assays for Determination of Acetyltransferase Activity and Specificity Using pNP-acetyl and Acetylated Polysaccharides as Substrates. *Bio-Protocol*, 4(3). doi:10.21769/bioprotoc.1037
31. Rancour DM, Marita JM, Hatfield RD (2012) Cell wall composition throughout development for the model grass *Brachypodium distachyon*. *Frontiers in plant science* 3: 266
32. Rancour DM, Hatfield RD, Marita JM, Rohr NA, Schmitz RJ (2015) Cell wall composition and digestibility alterations in *Brachypodium distachyon* achieved through reduced expression of the UDP-arabinopyranose mutase. *Plant Sci* 6: 446
33. Rennie, E. A., & Scheller, H. V. (2014). Xylan biosynthesis. *Current Opinion in Biotechnology* 26: 100-107
34. Sandler, J. D., & Joung, J. K. (2014). CRISPR-Cas Systems For Editing, Regulating, And Targeting Genomes. *Nature Biotechnology*, 32(4), april 2014, 347-355.
35. Sega, G. A. (1984). A review of the genetic effects of ethyl methanesulfonate. *Mutation Research/Reviews in Genetic Toxicology*, 134(2-3), 113-142. doi:10.1016/0165-1110(84)90007-1
36. Simmons, T. J., Mortimer, J. C., Bernardinelli, O. D., Pöppler, A., Brown, S. P., Deazevedo, E. R., Dupree, R., Dupree, P. (2016). Folding of xylan onto cellulose fibrils in plant cell walls revealed by solid-state NMR. *Nature Communications*, 7, 13902. doi:10.1038/ncomms13902
37. Sommer, A. (2015). Burning Fossil Fuels. *International Journal of Health Services*, 46(1), 48-52. doi:10.1177/0020731415625253
38. The Arabidopsis Genome Initiative. (2000). Analysis of the genome sequence of the flowering plant *Arabidopsis thaliana*. *Nature*, 408: 796-815
39. The International Brachypodium Initiative. (2010). Genome sequencing and analysis of the model grass *Brachypodium distachyon*. *Nature*, 463: 763-768
40. Tilman, D., Socolow, R., Foley, J.A., Hill, J., Larson, E., Lynd, L., Pacala, S., Reilly, J., Searchinger, T., Somerville, C., Williams, R. 2009, Beneficial Biofuels—The Food, Energy, and Environment Trilemma, *Science*, 325, July, 2009, 270-271
41. Urbanowicz, B. R., Pena, M. J., Ratnaparkhe, S., Avci, U., Backe, J., Steet, H. F., Foston, M., Li, H., O'Neill, M.A., Ragauskas, A.J., Darvill, A.G., Wyman, C., Gilbert, H.J., York, W. S. (2012). 4-O-methylation of glucuronic acid in *Arabidopsis* glucuronoxylan is catalyzed by a

- domain of unknown function family 579 protein. *Proceedings of the National Academy of Sciences*, 109(35), 14253-14258. doi:10.1073/pnas.1208097109
42. Vogel J (2008) Unique aspects of the grass cell wall. *Current opinion in plant biology* 11: 301-307
 43. Vogel, J., & Hill, T. (2007). High-efficiency Agrobacterium-mediated transformation of *Brachypodium distachyon* inbred line Bd21-3. *Plant Cell Reports*, 27(3), 471-478. doi:10.1007/s00299-007-0472-y
 44. Wall, P. K., Leebens-Mack, J., Muller, K. F., Field, D., Altman, N. S., & Depamphilis, C. W. (2007). PlantTribes: A gene and gene family resource for comparative genomics in plants. *Nucleic Acids Research*, 36(Database). doi:10.1093/nar/gkm972
 45. Weng, J., Li, X., Bonawitz, N. D., & Chapple, C. (2008). Emerging strategies of lignin engineering and degradation for cellulosic biofuel production. *Current Opinion in Biotechnology*, 19(2), 166-172. doi:10.1016/j.copbio.2008.02.014
 46. Withagen, C. (1994). Pollution and exhaustibility of fossil fuels. *Resource and Energy Economics*, 16(3), 235-242. doi:10.1016/0928-7655(94)90007-8
 47. Xie, K., Minkenberg, B., & Yang, Y. (2015). Boosting CRISPR/Cas9 multiplex editing capability with the endogenous tRNA-processing system. *Proceedings of the National Academy of Sciences*, 112(11), 3570-3575. doi:10.1073/pnas.1420294112
 48. Xie K, Zhang J and Yang Y. Genome-wide Prediction of Highly Specific Guide RNA Spacers for the CRISPR-Cas9 Mediated Genome Editing in Model Plants and Major Crops. *Mol. Plant*, 2014. doi: 10.1093/mp/ssu009
 49. Yamamoto, M., & Yamamoto, K. T. (1998). Differential Effects of 1-Naphthaleneacetic Acid, Indole-3-Acetic Acid and 2,4-Dichlorophenoxyacetic Acid on the Gravitropic Response of Roots in an Auxin-Resistant Mutant of *Arabidopsis*, aux1. *Plant and Cell Physiology*, 39(6), 660-664. doi:10.1093/oxfordjournals.pcp.a029419
 50. Yuan, Y., Teng, Q., Zhong, R., & Ye, Z. (2016). Roles of *Arabidopsis* TBL34 and TBL35 in xylan acetylation and plant growth. *Plant Science*, 243, 120-130. doi:10.1016/j.plantsci.2015.12.007

ACADEMIC VITA

Academic Vita of Justin Slovin

Email: jvs5934@gmail.com

Education

Major(s) and Minor(s): Major: Biology – vertebrate physiology option. Minor: Neuroscience

Honors: Completing Honors Thesis in biology

Thesis Title: Analyzing The Effects Of Disrupting Xylan Acetylation In *Brachypodium distachyon*

Thesis Supervisor: Dr. Charles Anderson

Work Experience:

Undergraduate research

Date: Fall 2015-present

Title: Undergraduate Research assistant

Description:

- Studying *Brachypodium distachyon* mutants and their growth patterns
- Analyzing the mutations to improve drought tolerance and biofuel production
- Researching pectin and its potential effects at reducing cancer cell metastasis (for past experiments not involved in this thesis)

Institution/Company (including location): Anderson Lab at Penn State University

Supervisor's Name: Dr. Charles T. Anderson

Medical Scribe

Date: Summer 2018 and beyond

Title: Medical Scribe

Description:

- Assisting physicians in completing patient examinations by recording notes, freeing up the physicians to connect with their patients on a more personal level.

Institution/Company (including location): ScribeAmerica at Children's Hospital Of Philadelphia

Presentations: Co-presented poster with another undergraduate at the summer 2017 CLSF conference

Community Service Involvement: Approximately 150 total hours of volunteer work split between Virtua Hospitals in Mt. Holly, NJ and Marlton, NJ.

Language Proficiency: English